

Analyzing brain structural differences among undergraduates with different grades of self-esteem using multiple anatomical brain network

Bo Peng (✉ pengbo@sibet.ac.cn)

SIBET, CAS, China

Gaofeng Pang

The Third Affiliated Hospital of Soochow University

Aditya Saxena

khandwa district hospital

Yan Liu

Suzhou Institute of Biomedical Engineering and Technology

Baohua Hu

Suzhou Institute of Biomedical Engineering and Technology

Suhong Wang

third affiliated hospital of soochow university

Yakang Dai

Suzhou Institute of Biomedical Engineering and Technology

Research

Keywords: structural magnetic resonance imaging, multi-resolution ROI, hierachal brain network, machine learning method, self-esteem

Posted Date: October 28th, 2020

DOI: <https://doi.org/10.21203/rs.3.rs-57459/v3>

License:  This work is licensed under a Creative Commons Attribution 4.0 International License.

[Read Full License](#)

Version of Record: A version of this preprint was published on February 12th, 2021. See the published version at <https://doi.org/10.1186/s12938-021-00853-z>.

Abstract

Background: Self-esteem is the individual evaluation of oneself. People with high self-esteem grade have mental health and can bravely cope with the threats from the environment. With the development of neuroimaging techniques, researches on the cognitive neural mechanisms of self-esteem are increased. Existing methods based on brain morphometry and single-layer brain network cannot characterize the subtle structural differences related to self-esteem.

Method: To solve this issue, we proposed multiple anatomical brain network framework based on multi-resolution ROI template to study the cognitive neuroscience mechanism of self-esteem. Multiple anatomical brain network consist of ROI features and hierachal brain network features extracted from structural MRI. For each layer, we calculated the correlation relationship between pairs of ROIs. In order to solve the high-dimensional problem caused by the large amount of network features, hybrid feature selection methods are adopted to reduce the number of features while retaining discriminative information to the maximum extent. Multi-kernel SVM is employed to integrate the various types of features by appropriate weight coefficient.

Result: The experimental results show that the proposed method can improve classification accuracy to 97.26% compared with single-layer brain network.

Conclusions: The proposed method provides a new perspective for the analysis of brain structure differences of self-esteem, which also has potential guiding significance in other researches involved brain cognitive activity and brain disease diagnosis.

Background

Self-esteem is regarded as self-affirmation and self-identification about oneself [1]. People with good mental health have a higher self-esteem grade and think of themselves as valuable persons [2]. Researchers found that undergraduates with high self-esteem grade feel that they deserve to be respected by others and are able to accept the individual's deficiencies [3]. While people with low self-esteem grade have low self-confidence and are more vulnerable to outside influences, which will result in low socioeconomic status and poor physical health. Neurophysiology research found that self-esteem composed of multiple subsystems that are structurally separated from each other but functionally interact [4]. Brain imaging studies suggest that self-esteem involves multiple psychological processes, including perception, memory, and introspection. These psychological processes have the corresponding brain regions. For example, self-face recognition related to the right brain, and autobiographical memory is mainly related to the hippocampus, and self-reference is associated with the medial prefrontal lobe [5]. In addition to these independent brain regions, self-esteem is also reflected in the brain network connection. Medial prefrontal cortex is activated during the process of social, self, and affective events [6]. Self-esteem has an important impact on their mental health and will also have impacts after it enters

social work. Therefore, in this study, we focus on exploring the differences between brain networks of undergraduates with different levels of self-esteem.

Brain network can reflect interaction of separated brain regions as a whole, which has an important role for a deep understanding of brain structures and cognitive neuroscience. The region of interest (ROI) are served as the node, and the correlation between brain regions are regarded as edge [7-8]. The definition of ROI is a key step in anatomical brain network analysis. Most existing methods use ROI-based methods to study brain structure and functional connections related to self-esteem. Kelly et al. use the functional near-infrared spectroscopy based cerebral blood flow imaging method to estimate the hemodynamic response function of each ROI, in order to study the brain networks that are activated during the processing of self-esteem [9]. Goldin et al. use functional magnetic resonance imaging (fMRI) to measure changes in the brain network between the self-esteem group and the self-confidence group by measuring the BOLD response in each ROI [10]. Chavez et al. conduct a psychophysiological interaction analysis to calculate the correlation between specific ROIs related to self-esteem [11]. Although a variety of neuroimaging methods can be used to explore the brain, structural magnetic resonance imaging (sMRI) is widely used due to its high imaging resolution for soft tissues [12]. Studies based on sMRI show that self-esteem involves multiple networks, including default mode networks and social cognition networks [13]. In addition, self-esteem dominated by bilateral brain and mainly controlled by right brain [14]. Although the above researches have initially revealed the brain structure of self-esteem, it only used single-layer network that cannot fully identify the subtle differences in network connectivity caused by self-esteem.

The motivation of this study is to use enhanced feature representation method to better examine brain structural connectivity related to self-esteem. In recent years, machine learning techniques become a research hotspot in the field of brain network analysis [8]. Brain network analysis can help us fully understand the cognitive psychological activity of self-esteem. However, there are few studies using machine learning methods to construct self-esteem related brain networks, especially for the construction of multi-layer brain networks. In this article, we propose multiple anatomical brain networks based on multi-resolution ROIs. The innovation of this method is to use the in-layer and between-layer connections to better describe the correlation between small brain regions and large brain functional areas, which improves the defects of single-layer brain network.

Results

Classification performance

In order to evaluate the classification performance of the proposed method, accuracy (ACC), sensitivity (SEN), specificity (SPE), area under the receiver operating characteristic curve (AUC), F score, balanced accuracy, Youden's index are used (Table 1). The research results show that the multi-layer brain network features have the highest classification accuracy of 97.26%, and the AUC is also greater than other feature types. This indicates that the multiple brain network features have advantages in characterizing structural differences among different self-esteem group. In addition, the higher specificity and sensitivity

also show that the multiple brain network features have better recognition capabilities in exploring the subtle differences in brain structure caused by self-esteem (Figure 1).

Weight coefficient

The role of the weight coefficient is to determine the proportion of the various types of features in the multi-kernel classifier (Figure 2). Appropriate weight coefficient helps on the best classifier performance. A smaller weight coefficient indicates that the contribution of the fourth-layer fine ROI features is lower, while the contribution of the hierarchical brain network features is higher. Through experiments, we can find the most suitable weight coefficient in the range of 0-1.

The weight coefficient has an important influence on the performance of the classifier. It is proved that the weight coefficient can make the classifier perform well in the relatively large range from 0.05 to 0.35, which can decline the difficulty of determining the ratio of the two features, which reflects the robustness of our proposed method. The best results are obtained at 0.05. At this time, the hierarchical brain network features contributed more to the classification than the high-resolution ROI features in the bottommost layer. This is because the hierarchical brain network can fully express the differences in brain structure between the two groups.

Top discriminative features

We use the proposed method to select the most discriminative ROI features (Figure 3). These ROIs include occipital lobe (superior and middle occipital gyrus, cuneus), frontal lobe (supplementary motor area, middle frontal gyrus), temporal lobe (middle temporal gyrus), parental lobe (precuneus, angular gyrus), limbic lobe (posterior cingulate gyrus), and central region (precentral gyrus). The experimental results also show that differences in brain structure related to self-esteem are mainly in white matter and cortical thickness (Table 2).

The top 15 network features selected from all four layers (Table 3). The most discriminative hierarchical network features are mainly distributed in limbic lobe and parental lobe (Figure 4).

Discussion

We studied multiple anatomical brain network related to self-esteem. Our results have demonstrated that the proposed method is superior to the single-layer network method. The multiple networks enhance the representation of the specific brain structure related to self-esteem, thereby providing an effective and novel method to detect self-esteem related biomarkers.

Improvement of the proposed method

It is difficult to fully understand the functional organization of the brain using only a single-layer network framework since the brain is a complex system. In this study, we construct a multiple anatomical brain network in multi-resolution ROIs to improve the classification performance. Compared with the single-

layer network based method, multiple networks enhance the classification performance by using supplementary information from different networks. Compared with the best results obtained using a single-layer network, our proposed multiple anatomical network method can improve the classification accuracy by 8.95% (Table 1).

Analysis of discriminative features

The discriminative ROI features discovered by our method are distributed in multiple regions of the brain. Because few current studies employ automatic classification method to study the brain structure of self-esteem, we only compare brain regions found through our machine learning method with existing morphological based studies. Compared with previous studies, our results showed consistency in departmental brain regions, including precuneus [4], precentral gyrus [15], middle frontal gyrus [16], cuneus [4], posterior cingulate [17]. This indicates the effectiveness of our classification method in revealing brain regions related to self-esteem. In addition to these consistent regions, we also found that the middle occipital, superior occipital, and supplementary motor are related to self-esteem. These brain regions have not been reported in previous studies.

The discriminative network features are mainly located on frontal, parietal and limbic lobe. After a comprehensive analysis of existing research on neuropsychological mechanisms related to self-esteem, we found that the frontal region is an important part of the neural basis related to self-esteem. The frontal lobe is responsible for self-evaluation, self-regulation, and emotion management. Individuals with low self-esteem have a stronger emotional response to social evaluations, while high self-esteem individuals show stronger self-positivity in the process of self-evaluation. These findings indicate that frontal lobe plays an important role in generating positive self-information.

Comparison with other methods

Since few studies have used machine learning to analyze the relationship between self-esteem and brain structure, we compare our results with the current morphological studies related to self-esteem. At present, most studies have found a correlation between self-esteem and frontal lobe [6, 16, 17]. The frontal lobe is mainly responsible for the cognitive activities of the brain, and self-esteem involves cognitive processing and emotional response. The results of this paper are generally consistent with those of previous studies. In addition, some specific brain regions, such as the cuneus, have been found to be related to many self-related functions, such as self-related information processing and various aspects of consciousness [16]. In addition, we also found a correlation between cingulate cortex and self-esteem. Studies have shown that when individuals are accepted by society, individuals activate the ventral anterior cingulate cortex and medial prefrontal cortex, thus enhancing self-esteem [17]. Therefore, the study of brain structure with different self-esteem grades is helpful to understand the neurophysiological mechanism of self-esteem.

At the same time, in order to prove the effectiveness of the proposed method. We have compared the classification performance with different classifiers. Table 4 shows the classification results using

different classifies. The results show that the proposed method based on multiple anatomical brain networks has better performance than all the other classifiers.

Limitations and future directions

Although the classification performance is good, our study still has some limitations. Here, we put forward some future directions in order to conduct a better research on self-esteem in cognitive neuroscience. First, as a preliminary study, we use relatively small amount data in machine learning. In the follow-up study, we will collect more data, taking psychological, individual, and social factors into account, and make a more detailed grades of self-esteem. Second, other metrics for modeling the interactions between ROIs, such as Euclidean distance and the L_1 -norm distance measure. Third, with the increasing of the data, deep learning can also be used to automatically extract features to find the discriminative features of multiple brain network, such as depth automatic encoder. Fourth, due to the multi types of features involved in this study, multiple weight factors can be used for better feature fusion.

Conclusions

In this study, we have presented how multiple anatomical brain networks can be used to analyze brain structural differences among undergraduates with different grades of self-esteem. Hybrid feature selection methods are adopted to reduce the number of features, and multi-kernel SVM was employed to integrate various types of features by appropriate weight coefficient. The features extracted from these networks can be used to improve the defects that the traditional single-layer brain network contains insufficient information. The experiments show that our method has improved performance compared with the single-layer network structure, which can provide a new perspective for the analysis of brain structure differences of self-esteem. It also has potential guiding significance in other researches involved brain cognitive activity and brain disease diagnosis.

Methods

Subjects

The structural sMRI data used in our study were acquired from the Soochow University, which is composed of 68 undergraduates. The study was approved by the Ethics Committee of the Third Affiliated Hospital of Soochow University. Written informed consents was obtained from all subjects. All subjects have not received stimulants or hypnotics before acquisition in order to keep them awake and let the brain work normally. All participants' vision was normal or corrected to normal, and they were right-handed. After the test, each participant will receive a small gift or financial reward. All subjects are required to perform Rosenberg Self-esteem Scale (RSES) test. The RSES is originally developed by Rosenberg in 1965 to assess the overall feelings of undergraduates about self-worth and self-acceptance. It is the most used self-esteem measurement tool in the psychology community [18]. We

ranked the RSES test scores from highest to lowest, and then divided them into two groups: high self-esteem group and low self-esteem group. Table 5 provides detailed information of all participants.

Imaging acquisition and preprocessing

All images were collected on a 3T Siemens Medical Systems equipment. The acquisition parameters are set as: echo time (TE) = 2.98 ms, repetition time (TR) = 2300 ms, flip angle (FA) = 9 deg, voxel size = $1 \times 1 \times 1$ mm³, slice thickness = 1 mm, field of view (FoV) = 256mm.

We use an automatic pipeline for sMRI image processing. Firstly, image preprocessing is conducted to remove the gray-scale unevenness of the image and adjust the image orientation to match the template [19]. Secondly, brain extraction is performed to remove the non-brain tissue, such as the skull and cerebellum [20]. Thirdly, gray matter (GM), white matter (WM) and cerebrospinal fluid (CSF) were segmented from the background [21]. Fourth, the segmented image was registered to the template labeled with the Automated Anatomical Labeling (AAL) template [22]. Fifth, in order to calculate the morphological features based on the cortex, the middle layer of the cerebral cortex was depicted [23]. After the whole processing, the morphological measurements of GM volume, WM volume, CSF volume, cortical thickness, and cortical surface area of each ROI were obtained for each subject. It should be noted that we removed 12 subcortical ROIs from AAL template considering that the cerebral cortex contains more neurons.

Classification framework

The framework of the proposed classification algorithm based on multi-resolution ROI brain network is shown in Figure 5, mainly including multiple anatomical network construction, feature selection, and classification. Multi-resolution ROI based multiple anatomical brain network were constructed based on morphological features (volume of different brain tissue, cortical thickness, and cortical surface area). Feature selection can reduce the dimensionality of high-dimensional brain network features, only retaining the features that can maximize the specificity of the subjects. The optimal feature subset can be trained by the classifier as neuroimaging markers representing different self-esteem levels.

Construction of multiple anatomical networks

Through the above image processing steps, GM volume, WM volume, CSF volume, cortical thickness, and cortical surface area of each ROI can be obtained from the MRI image of each subject. In order to reduce individual differences, standardization was performed, dividing the measured value of each ROI by the total intracranial volume, mean cortical thickness, and whole cerebral cortical surface area of the subject. Therefore, we used normalized volume and cortical features to provide a more appropriate representation. More objective measurements can be received by such processing. In order to improve the performance of the classifier, we propose a four-layer hierarchical network framework in this paper. We used brain templates with different ROI resolution in each layer to construct brain network nodes and edges.

Specifically, the bottommost template containing 78 ROIs is defined L^4 , the remaining three layers are defined as L^l , where $l = 1, 2, 3$. A larger l value indicates a higher-resolution ROI, which is located in the brain network layer closer to the bottom of the hierarchy. By merging small brain regions into large brain functional areas, the number of ROIs are reduced. In the layer L^3 , there are 36 ROIs by dividing the whole brain into lateral, medial and inferior surfaces. In the layer L^2 , 14 ROIs are defined reflecting to the anatomical brain structure of central, frontal, parietal, occipital, temporal, limbic, and insula lobe. The specific definition rules of these ROIs can be found in Table 6. It is worth noting that in the first layer L^1 , we study the brain as a whole.

For each layer, correlation between ROIs can be calculated using brain template defined above. Its node correspond to the ROIs in different resolution, and the edge corresponds to the interaction between pairs of ROIs. Take the bottom layer L^4 as an example, an 78×78 matrix C^4 can be calculated by computing the Pearson correlation coefficient between the i -th ROI and j -th ROI. We define

$$C^4(i, j) = \exp \left\{ -\frac{[t(i) - t(j)]^2}{2\sigma^2} \right\} \quad (1)$$

Where $t^{(i)}$ and $t^{(j)}$ represent the mean thickness of the cerebral cortex corresponding to the i -th and j -th ROIs.

σ is defined as $\sigma = \sqrt{\sigma_i^2 + \sigma_j^2}$, where σ_i and σ_j represent the standard deviation of cortex for the i -th and j -th ROI. Due to the symmetry of the correlation matrix, we only use the upper triangular elements of the matrix C^4 to construct the feature vector. We connect the 3003 upper triangular elements to form the corresponding feature vector for L^4 . Since the ROIs in the remaining three layers are obtained by merging ROIs in the bottommost layer, the mean and standard deviation of these compound ROIs can be obtained by calculating the average value of all ROIs. The definition of correlation matrix C^l for other layers is similarly to C^4 . The union of the hierarchical networks is constructed by junction of the four upper triangular correlation matrix into a long vector.

Feature selection

In order to reduce the feature dimension and filter out the most discriminative features, we adopted a hybrid feature selection method. First, we use the statistical t-test method for preliminary selection of features with the significant p value less than the threshold ($p < 0.05$). Then, the redundant features are removed using the minimum redundancy and maximum correlation (mRMR) method, and only the features that can express the difference between groups in the minimum number are retained [24]. After the above two filter-based feature selections, the machine learning recursive feature elimination (SVM-RFE) method [25] is used to further reduce the feature dimension. After completing the entire feature selection steps, the optimal feature subset is obtained.

Classification using multi-kernel SVM

There are various types of features in the multiple brain network, one is the high-resolution ROI features in the fourth layer, and the other is the brain network features corresponding to different layers. Multi-kernel machine learning method can integrate these various types of features into a final classifier. Firstly, a Gaussian Radial Basis Function (RBF) kernel function is used to construct a kernel matrix for each type of feature. Secondly, the two kernel matrices are integrated into the multi-kernel matrix through appropriate weight coefficients [25]. Comparing the results of using linear kernel function and using RBF function (non-linear), we discover that the RBF kernel can significantly improve the classification performance. Therefore, we choose the RBF kernel function to construct the multi-kernel classifier. Finally, the optimal features subset can be obtained.

Cross-validation

The nested cross-validation method has been applied in our previous research [26]. In the inner loop, the training set are used to determine the parameters of the classifier. In the outer loop, the testing set is used to evaluate the generalization ability of the classifier. It should be noted that at the beginning of the experiment, the entire data set was randomly divided into two parts, one for training and the other one for testing. The training set and testing set can be exchanged throughout the verification process, while the processing steps remain unchanged.

Abbreviations

ROI: the region of interest; fMRI: functional magnetic resonance imaging; sMRI: structural magnetic resonance imaging; RSES: Rosenberg Self-esteem Scale; TE: echo time; TR: repetition time; FA: flip angle; FoV: field of view; GM: gray matter; WM: white matter; CSF: cerebrospinal fluid; AAL: Automated Anatomical Labeling; mRMR: the minimum redundancy and maximum correlation; SVM-RFE: the machine learning recursive feature elimination; RBF: Radial Basis Function.

Declarations

Acknowledgements

The authors would like to thank the physicians in department of neuroscience, the Third Affiliated Hospital of Soochow University for their help collecting the brain MR images of the young adults with different self-esteem scales.

Author's contributions

Suhong Wang contributed to the conception of the study. Aditya Saxena performed the experiment. Yakang Dai and Bo Peng contributed significantly to analysis and manuscript preparation. Bo Peng performed the data analyses and wrote the manuscript. Yan Liu and Baohua Hu helped perform the analysis with constructive discussions.

Funding

This work was supported by National Key Research and Development Plan (2018YFC0116904, 2017YFC0114304, 2017YFB1103602), National Natural Science Foundation of China (61801476), Scientific Research Equipment Program of Chinese Academy of Science (YJKYYQ20170050), Jiangsu Key Technology Research Development Program (BE2016613, BE2017675, BE2017663, BE2018610, BE2017664), Jiangsu Natural Science Foundation (BK20170387, BK20180221), Zhejiang Key Technology Research Development Program (2018C03024), Suzhou Industry Technological Innovation Projects (SYG201606, SYG201707), Suzhou Science & Technology Projects for People's Livelihood (SS201866, SYS2018010, SS201854, SS201855), Suzhou Science and Technology Development Project (Szs201609, Szs201818), Lishui Key Technology R&D Program (2019ZDYF17, 2019ZDYF09), SIBET Medical and Technology Project (Y853111305, Y853171305), SND Medical Plan Project (2016Z010, 2017z005).

Availability of data and materials

The datasets used and/or analyzed during the current study are available from the corresponding author on reasonable request.

Ethics approval and consent to participate

The study is approved by the Ethics Committee of the Third Affiliated Hospital of Soochow University.

Consent for publication

All subjects gave written informed consent in accordance with the Declaration of Helsinki.

Competing interests

The authors declare that they have no competing interests.

References

1. Saiphoor AN, Halevi LD, Vahedi Z. Social networking site use and self-esteem: A meta-analytic review. *Personality and Individual Differences*. 2020;153:109639.
2. Rieger S, Göllner R, Trautwein U, et al. Low self-esteem prospectively predicts depression in the transition to young adulthood: A replication of Orth, Robins, and Roberts. *Journal of personality and social psychology*. 2016;110(1):e16.
3. Chavez RS, Heatherton TF. Structural integrity of frontostriatal connections predicts longitudinal changes in self-esteem. *Social neuroscience*. 2017;12(3):280-286.
4. Zilverstand A, Huang AS, Alia-Klein N, et al. Neuroimaging impaired response inhibition and salience attribution in human drug addiction: a systematic review. *Neuron*. 2018;98(5):886-903.

5. Wang Y, Zhang L, Kong X, et al. Pathway to neural resilience: Self-esteem buffers against deleterious effects of poverty on the hippocampus. *Human brain mapping*. 2016;37(11):3757-3766.
6. Lieberman MD, Straccia MA, Meyer ML, et al. Social, self,(situational), and affective processes in medial prefrontal cortex (MPFC): Causal, multivariate, and reverse inference evidence. *Neuroscience & Biobehavioral Reviews*. 2019;99:311-328.
7. Bede P, Hardiman O. Longitudinal structural changes in ALS: a three time-point imaging study of white and gray matter degeneration. *Amyotrophic Lateral Sclerosis and Frontotemporal Degeneration*. 2018;19(3-4):232-241.
8. Solé-Casals J, Serra-Grabulosa JM, Romero-Garcia R, et al. Structural brain network of gifted children has a more integrated and versatile topology. *Brain Structure and Function*. 2019;224(7):2373-2383.
9. Kelley WM, Macrae CN, Wyland CL, et al. Finding the self? An event-related fMRI study. *Journal of cognitive neuroscience*. 2002;14(5):785-794.
10. Goldin P, Ziv M, Jazaieri H, et al. Randomized controlled trial of mindfulness-based stress reduction versus aerobic exercise: effects on the self-referential brain network in social anxiety disorder. *Frontiers in human neuroscience*. 2012;6:295.
11. Cuingnet R, Gerardin E, Tessieras J, et al. Automatic classification of patients with Alzheimer's disease from structural MRI: a comparison of ten methods using the ADNI database. *Neuroimage*. 2011;56(2):766-781.
12. Schmitgen MM, Niedtfeld I, Schmitt R, et al. Individualized treatment response prediction of dialectical behavior therapy for borderline personality disorder using multimodal magnetic resonance imaging. *Brain and Behavior*. 2019;9(9):e01384.
13. Erol RY, Orth U. Self-esteem development from age 14 to 30 years: A longitudinal study. *Journal of personality and social psychology*. 2011;101(3):607.
14. Peng B, Saxena A, Wang S, et al. Enhancing the Representation of Multiple Anatomical Network for Young Adults with Self-Esteem Difference. 2019 12th International Congress on Image and Signal Processing, BioMedical Engineering and Informatics (CISP-BMEI). IEEE. 2019;1-5.
15. Cheng W, Rolls ET, Qiu J, et al. Functional connectivity of the precuneus in unmedicated patients with depression. *Biological Psychiatry: Cognitive Neuroscience and Neuroimaging*. 2018;3(12):1040-1049.
16. Yang J, Xu X, Chen Y, et al. Trait self-esteem and neural activities related to self-evaluation and social feedback. *Scientific reports*. 2016;6(1):1-10.
17. Van Schie CC, Chiu CD, Rombouts SARB, et al. When compliments do not hit but critiques do: an fMRI study into self-esteem and self-knowledge in processing social feedback. *Social Cognitive and Affective Neuroscience*. 2018;13(4):404-417.
18. García JA, y Olmos FC, Matheu ML, et al. Self esteem levels vs global scores on the Rosenberg self-esteem scale. *Heliyon*. 2019;5(3):e01378.
19. Thirion JP. Image matching as a diffusion process: an analogy with Maxwell's demons. 1998.
20. Smith SM. Fast robust automated brain extraction. *Human brain mapping*. 2002;17(3):143-155.

21. Wang L, Shi F, Li G, et al. 4D segmentation of brain MR images with constrained cortical thickness variation. *PLoS one*. 2013;8(7):e64207.
22. Tzourio-Mazoyer N, Landeau B, Papathanassiou D, et al. Automated anatomical labeling of activations in SPM using a macroscopic anatomical parcellation of the MNI MRI single-subject brain. *Neuroimage*. 2002;15(1):273-289.
23. Li G, Wang L, Yap P T, et al. Computational neuroanatomy of baby brains: A review. *NeuroImage*. 2019;185:906-925.
24. Peng H, Xie P, Liu L, et al. Brain-wide single neuron reconstruction reveals morphological diversity in molecularly defined striatal, thalamic, cortical and claustral neuron types. *bioRxiv*. 2020;675280.
25. Sanz H, Valim C, Vegas E, et al. SVM-RFE: selection and visualization of the most relevant features through non-linear kernels. *BMC bioinformatics*. 2018;19(1):1-18.
26. Peng B, Lu J, Saxena A, et al. Examining brain morphometry associated with self-esteem in young adults using multilevel-ROI-features-based classification method. *Frontiers in Computational Neuroscience*. 2017;11:37.

Tables

Table 1. Classification performance using different feature types.

	ACC (%)	AUC (%)	SEN (%)	SPE (%)	Y (%)	F (%)	BAC (%)
Network features in the 4th layer	90.69	96.63	87.72	90.65	86.74	77.38	88.77
Network features in the 3th layer	88.31	84.27	85.32	84.29	88.33	82.62	85.74
Network features in the 2th layer	89.59	76.65	78.53	75.94	73.24	69.18	67.77
Network features in all layers	92.59	91.93	91.51	90.91	93.27	87.18	91.49
ROI features in the 4th layer	88.69	85.63	87.72	87.65	86.74	77.38	88.77
ROI features and network features in the 4th layer	94.41	95.58	94.42	93.41	92.47	92.82	92.64
Multilevel (ROI features in the 4th layer and network features in all layers)	97.26	99.88	97.27	97.41	97.12	94.53	97.27

* ACC = accuracy; AUC = area under receiver operating characteristic curve; SEN = sensitivity; SPE = specificity; Y = Youden's index; F = F-score; BAC = Balanced accuracy.

Table 2. Top 15 most discriminating regional features that were selected using the proposed classification framework.

No.	Name of ROI	L/R	Tissue	Brain Lobe	Frequency
1	Middle frontal gyrus	R	WM	Frontal lobe	185
2	Superior occipital gyrus	R	GM	Occipital lobe	144
3	Precentral gyrus	R	Thickness	Central region	141
4	Middle occipital gyrus	L	GM	Occipital lobe	102
5	Supplementary motor area	R	WM	Frontal lobe	86
6	Posterior cingulate gyrus	L	CSF	Limbic lobe	75
7	Middle frontal gyrus	L	WM	Frontal lobe	73
8	Posterior cingulate gyrus	L	Thickness	Limbic lobe	70
9	Middle occipital gyrus	R	Thickness	Occipital lobe	68
10	Angular gyrus	R	WM	Parietal lobe	64
11	Precuneus	R	Thickness	Parietal lobe	58
12	Cuneus	L	WM	Occipital lobe	58
13	Middle temporal gyrus	L	Area	Temporal lobe	54
14	Precuneus	L	Thickness	Parietal lobe	53
15	Middle occipital gyrus	L	Thickness	Occipital lobe	53

L = left hemisphere; R = right hemisphere; GM = gray matter volume; WM = white matter volume; CSF = cerebrospinal volume; Thickness = cortical thickness; Area = cortical surface area; Frequency = selected frequency over 100 repetitions of two-fold cross validation.

Table 3. Top 15 similarity features that were selected using the proposed classification framework.

Network	Name of ROI	L/R	Name of ROI	L/R	No.	Frequency
Network 4	Orbitofrontal cortex (inferior)	L	Superior parietal gyrus	L	15	45
	Rectus gyrus	L	Precuneus	L	12	48
	Orbitofrontal cortex (inferior)	L	Paracentral lobule	R	10	54
	Orbitofrontal cortex (inferior)	R	Precuneus	L	3	95
Network 3	Parietal lobe: Lateral surface	R	Limbic lobe: Temporal pole (superior)	R	1	118
	Frontal lobe: Lateral surface	L	Parietal lobe: Lateral surface	L	2	114
	Temporal lobe: Lateral surface	L	Parietal lobe: Lateral surface	R	4	93
	Frontal lobe: Lateral surface	R	Temporal lobe: Lateral surface	R	5	93
	Frontal lobe: Lateral surface	R	Parietal lobe: Lateral surface	L	6	92
	Central region: Rolandic operculum	L	Limbic lobe: Temporal pole (superior)	L	7	74
	Central region: Postcentral gyrus	R	Parietal lobe: Lateral surface	R	9	61
	Temporal lobe: Lateral surface	R	Limbic lobe: Temporal pole (superior)	R	13	47
	Parietal lobe: Lateral surface	L	Limbic lobe: Temporal pole (superior)	L	14	47
Network 2	Central region	L	Limbic lobe	L	8	73
	Central region	R	Limbic lobe	L	11	54

L = left hemisphere; R = right hemisphere; Frequency = selected frequency over 100 repetitions of two-fold crossvalidation.

Table 4. The classification results using different classifiers.

Configurations	Classification accuracy (%)
SVM (RBF)	97.27
SVM (linear)	97.07
K-nearest neighbor classifier	94.25
Naive Bayes classifier	92.13
Decision tree algorithm	91.19

Table 5. Demographic information of all subjects

	High self-esteem group	Low self-esteem group	p value
Subjects	34	34	
Male/Female	19/15	16/18	0.83
Age (mean±SD)	21.90±1.16	22.53±1.42	0.77
Rosenberg Scale (mean±SD)	25.35±0.81	17.86±3.35	<0.001

The *p*-value of gender was obtained by chi-squared test.

The *p*-values of age and Rosenberg scale were obtained by *t*-test

Significance level was set to 0.05

Table 6. Regions of interest (ROIs) defined in the automated anatomical labeling (AAL) template.

Network 2		Network 3		Network 4	
No.	Name of ROI	No.	Name of ROI	No.	Name of ROI
1, 2	Central region	1, 2	Central region: Precentral gyrus	1, 2	Precentral gyrus
		3, 4	Central region: Postcentral gyrus	53, 54	Postcentral gyrus
		5, 6	Central region: Rolandic operculum	17, 18	Rolandic operculum left
3, 4	Frontal lobe	7, 8	Frontal lobe: Lateral surface	3, 4	Superior frontal gyrus (dorsal)
				7, 8	Middle frontal gyrus
				11, 12	Inferior frontal gyrus (opercular)
				13, 14	Inferior frontal gyrus (triangular)
		9, 10	Frontal lobe: Medial surface	19, 20	Supplementary motor area
				23, 24	Superior frontal gyrus (medial)
				65, 66	Paracentral lobule
		11, 12	Frontal lobe: Orbital surface	5, 6	Orbitofrontal cortex (superior)
				9, 10	Orbitofrontal cortex (middle)
				15, 16	Orbitofrontal cortex (inferior)
				21, 22	Olfactory
5, 6	Temporal lobe	13, 14	Temporal lobe: Lateral surface	25, 26	Orbitofrontal cortex (medial)
				27, 28	Rectus gyrus
				67, 68	Heschl gyrus
				69, 70	Superior temporal gyrus
7, 8	Parietal lobe	15, 16	Parietal lobe: Lateral surface	73, 74	Middle temporal gyrus
				77, 78	Inferior temporal gyrus
				55, 56	Superior parietal gyrus
				57, 58	Inferior parietal lobule
9, 10	Occipital lobe	17, 18	Parietal lobe: Medial surface	59, 60	Supramarginal gyrus
				61, 62	Angular gyrus
				63, 64	Precuneus
				45, 46	Superior occipital gyrus
		21, 22	Occipital lobe: Medial and inferior surfaces	47, 48	Middle occipital gyrus
				49, 50	Inferior occipital gyrus
				39, 40	Calcarine cortex
				41, 42	Cuneus
11, 12	Limbic lobe	23, 24	Limbic lobe: Temporal pole (superior)	43, 44	Lingual gyrus
			Limbic lobe: Temporal pole (middle)	51, 52	Fusiform gyrus
			Limbic lobe: Anterior cingulate gyrus	71, 72	Temporal pole (superior)
			Limbic lobe: Middle cingulate gyrus	75, 76	Temporal pole (middle)
			Limbic lobe: Posterior cingulate gyrus	31, 32	Anterior cingulate gyrus
			Limbic lobe: ParaHippocampal gyrus	33, 34	Middle cingulate gyrus
13, 14	Insula	35, 36	Insula: Insula	35, 36	Posterior cingulate gyrus
				37, 38	ParaHippocampal gyrus
				29, 30	Insula

Figures

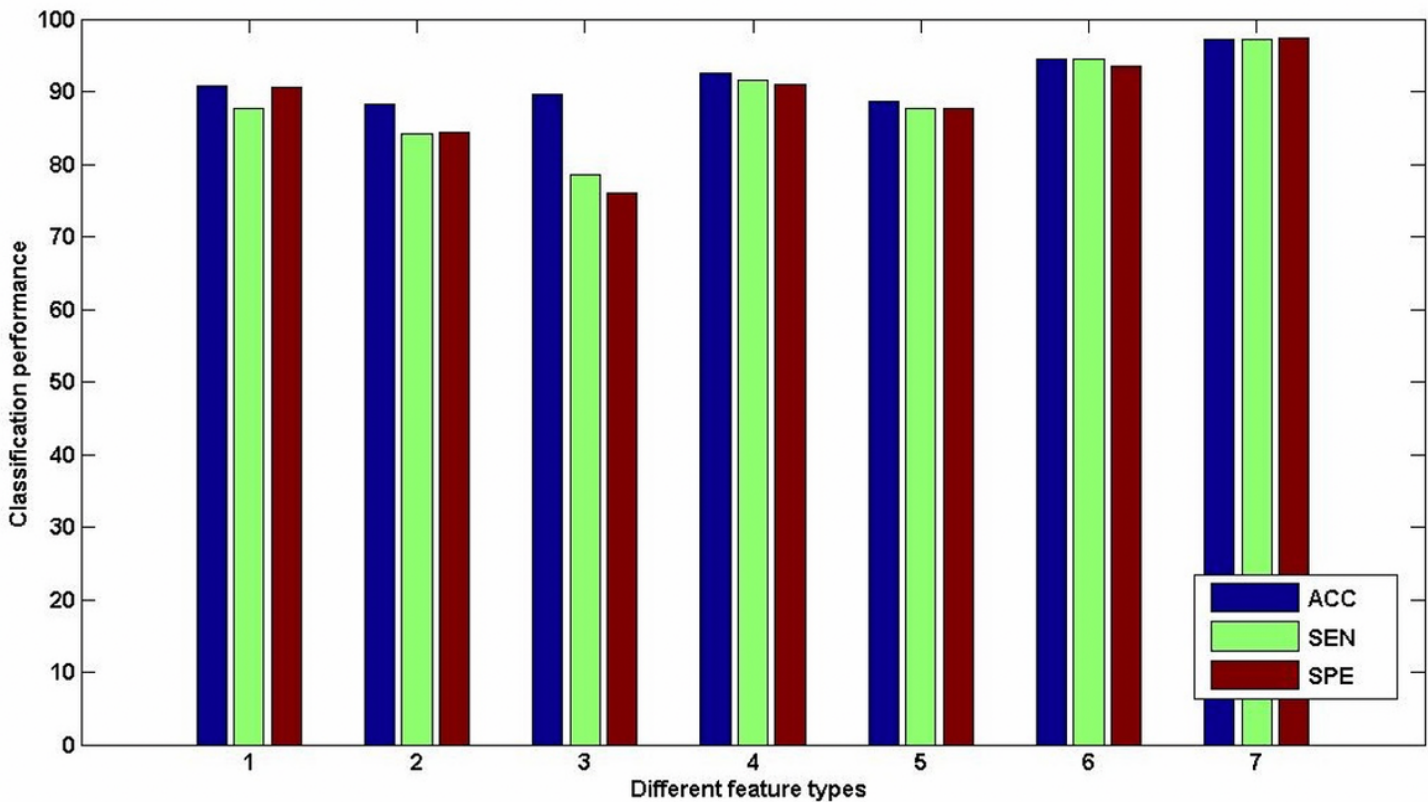


Figure 1

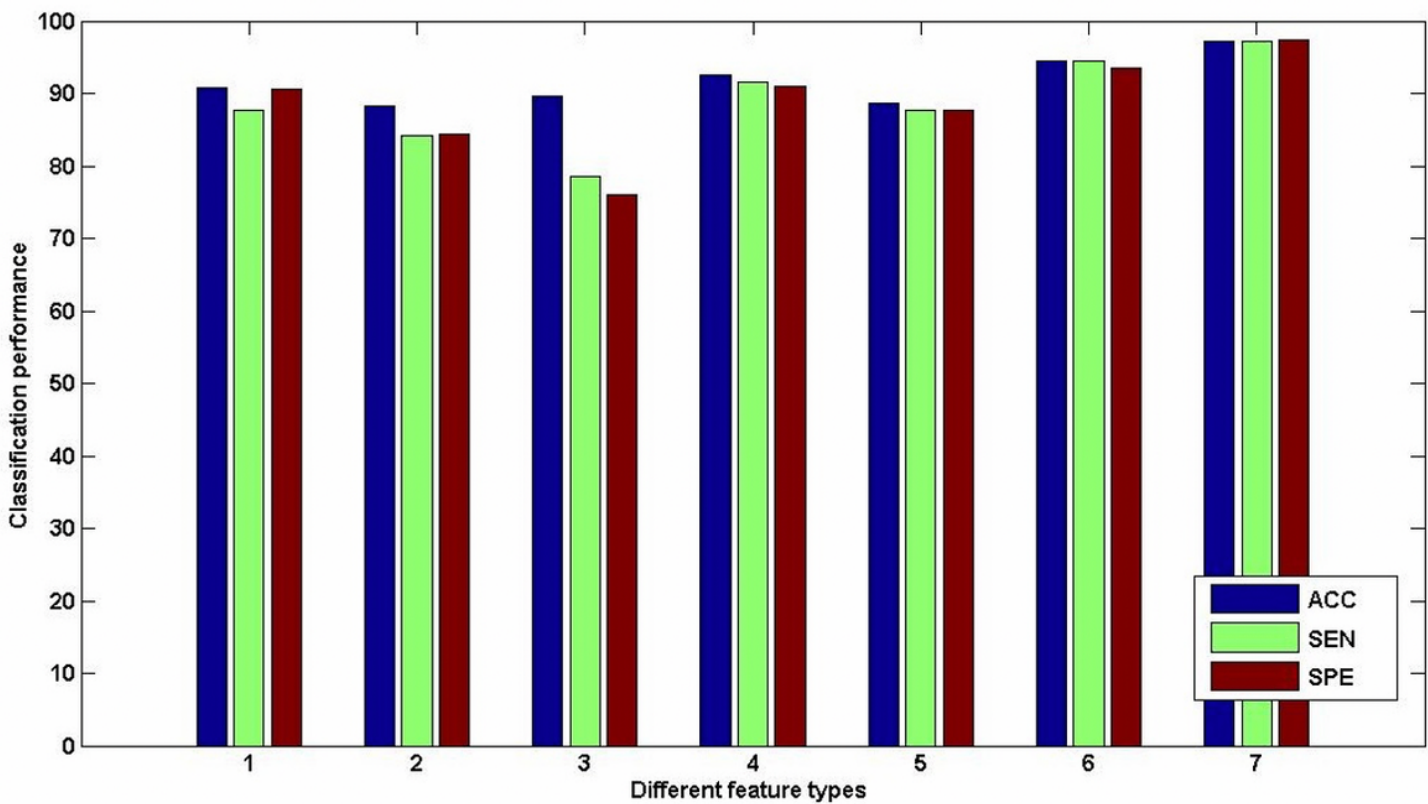


Figure 2

Boxplot of classification accuracy for different feature types. (1) Network features in the 4th layer, (2) Network features in the 3th layer, (3) Network features in the 2th layer, (4) Network features in all layers, (5) ROI features in the 4th layer, (6) ROI features and network features in the 4th layer, (7) Multilevel features. ACC = accuracy, SEN = sensitivity, SPE = specificity.

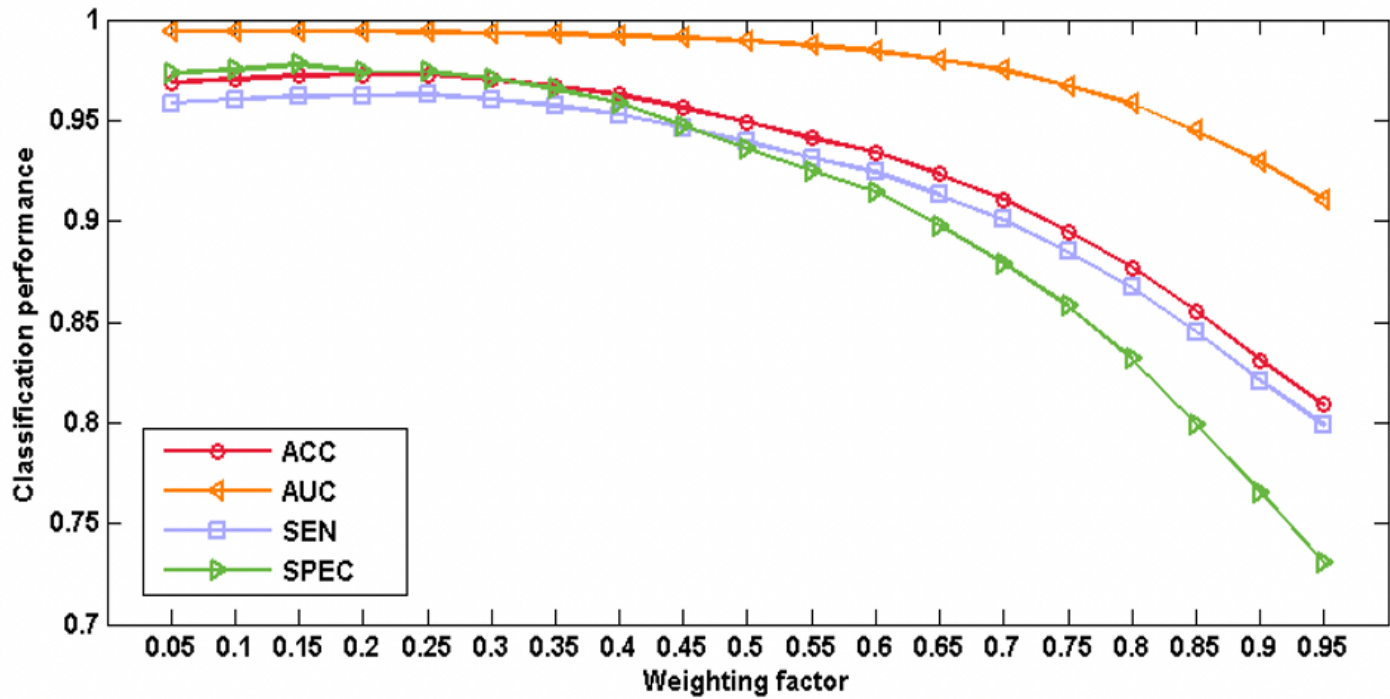


Figure 3

Classification performance with multilevel ROI features using different weighting factors. The weight for the ROI features decrease from left to right (range from 0 to 1).

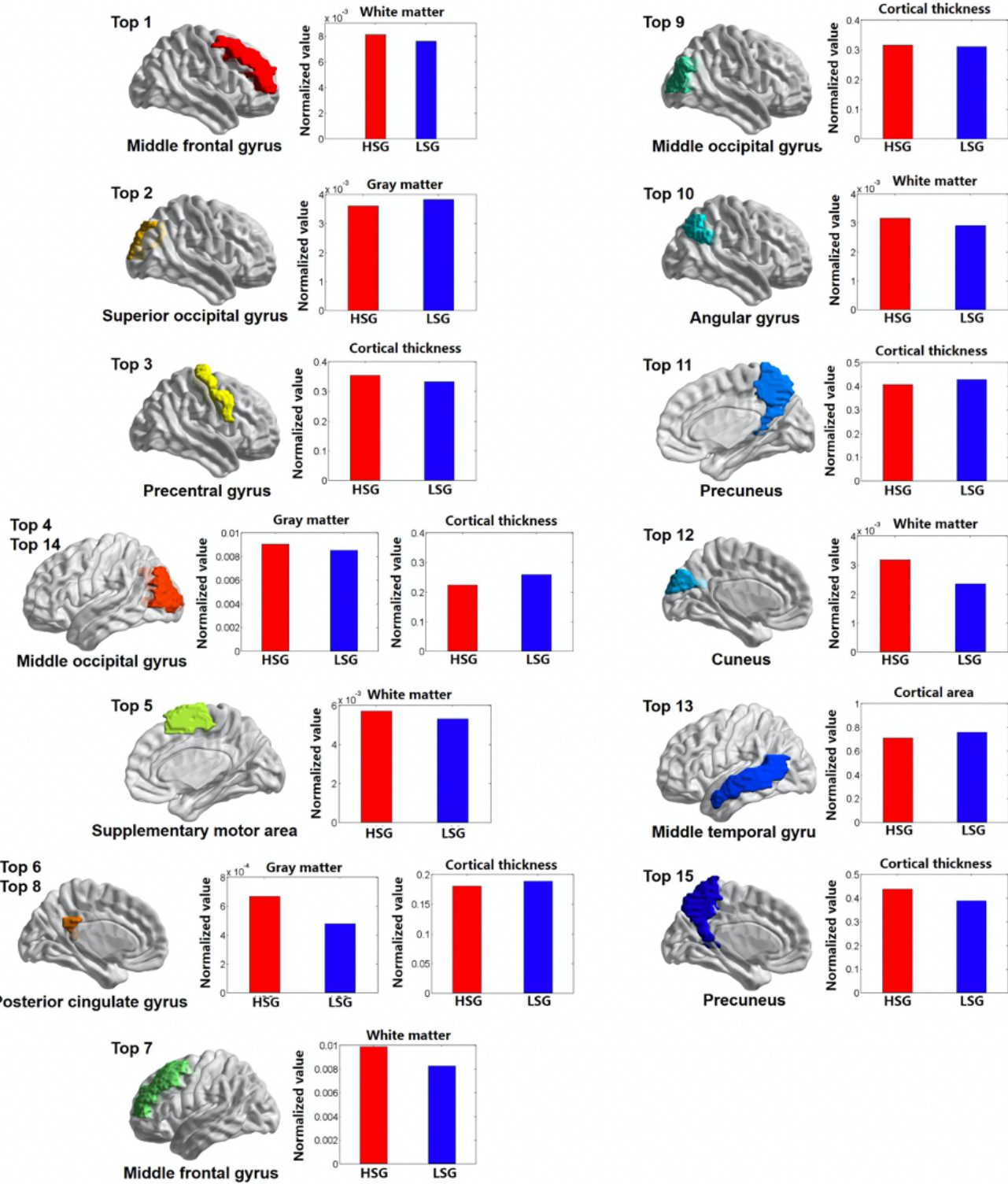


Figure 4

The most discriminating ROI features projected onto the cortical surface. HSG means high self-esteem group and LSG means low self-esteem group.

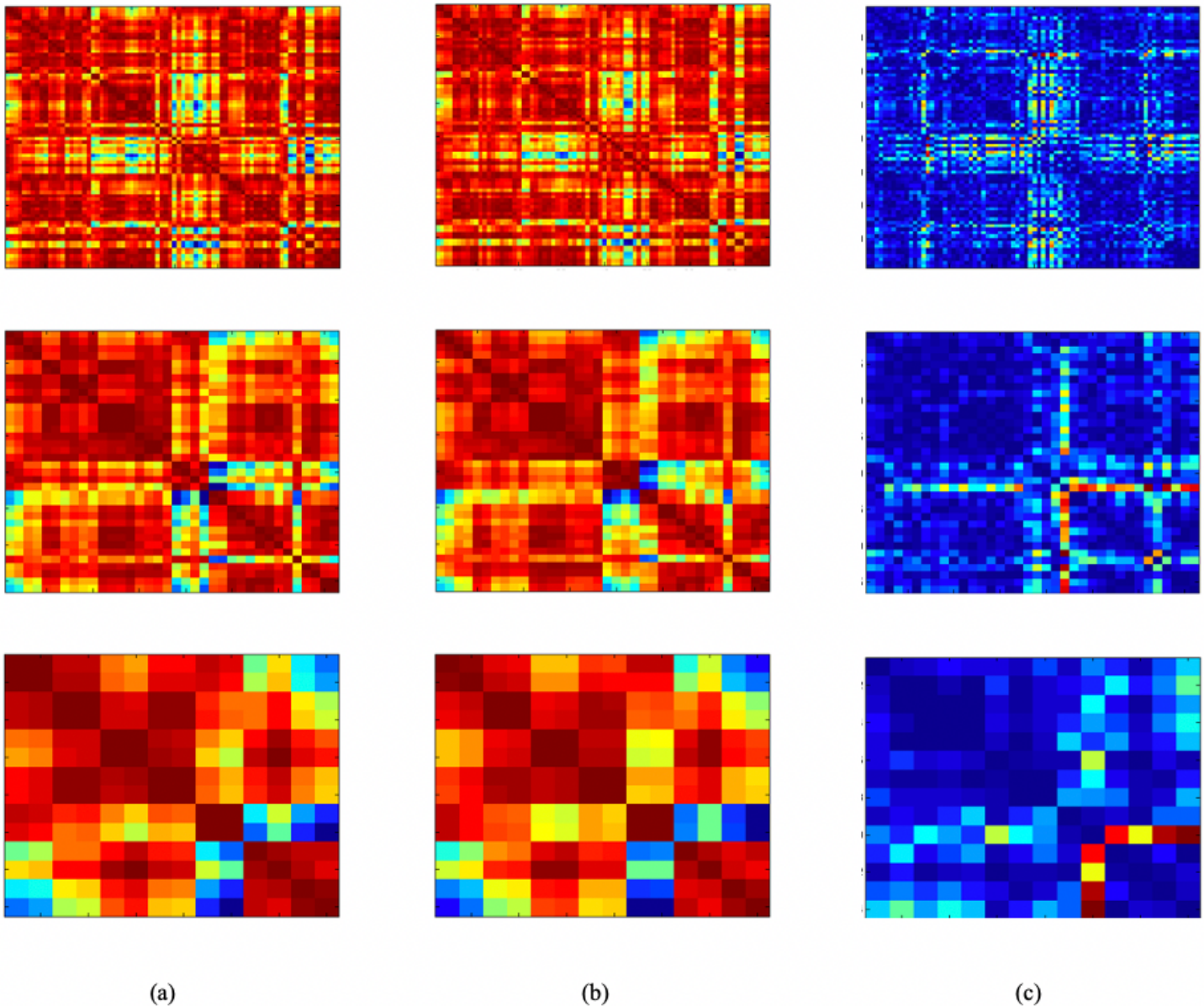


Figure 5

Correlative matrix. (a) high self-esteem group, (b) low self-esteem group. (c) differences between the two groups.

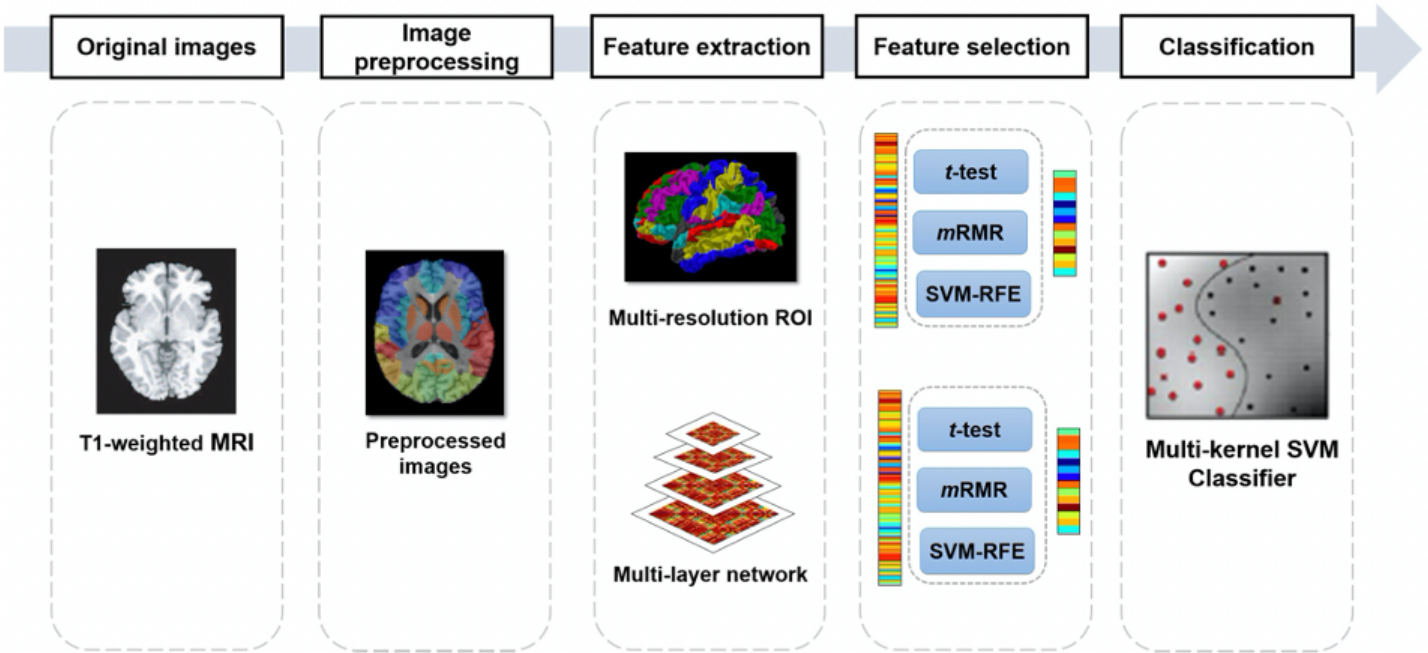


Figure 6

Framework of the classification method using multilevel network features.